Energies **2013**, *6*, 6352-6372; doi:10.3390/en6126352

OPEN ACCESS

energies

ISSN 1996-1073

www.mdpi.com/journal/energies

Article

Effect of Tower Shadow and Wind Shear in a Wind Farm on AC Tie-Line Power Oscillations of Interconnected Power Systems

Jin Tan [1], Weihao Hu [2], Xiaoru Wang [1,*] and Zhe Chen [2]

[1] School of Electrical Engineering, Southwest Jiaotong University, Chengdu 610031, China; E-Mail: tanjin570111@163.com

[2] Department of Energy Technology, Aalborg University, Pontoppidanstraede 101, Aalborg DK-9220, Denmark; E-Mails: whu@et.aau.dk (W.H.); zch@et.aau.dk (Z.C.)

* Author to whom correspondence should be addressed; E-Mail: xrwang@home.swjtu.edu.cn; Tel./Fax: +86-28-8760-1128.

Received: 4 November 2013; in revised form: 27 November 2013 / Accepted: 28 November 2013 / Published: 4 December 2013

Abstract: This paper describes a frequency domain approach for evaluating the impact of tower shadow and wind shear effects (TSWS) on tie-line power oscillations. A simplified frequency domain model of an interconnected power system with a wind farm is developed. The transfer function, which relates the tie-line power variation to the mechanical power variation of a wind turbine, and the expression of the maximum magnitude of tie-line power oscillations are derived to identify the resonant condition and evaluate the potential risk. The effects of the parameters on the resonant magnitude of the tie-line power are also discussed. The frequency domain analysis reveals that TSWS can excite large tie-line power oscillations if the frequency of TSWS approaches the tie-line resonant frequency, especially in the case that the wind farm is integrated into a relatively small grid and the tie-line of the interconnected system is weak. Furthermore, the results of the theoretical analysis are validated through time domain simulations conducted in the two-area four-generator system and the Western Electric Coordinating Council 127 bus system.

Keywords: wind power integration; interconnected power systems; tie-line power oscillations; forced power oscillation; low frequency oscillations; tower shadow and wind shear (TSWS)

---

1. Introduction

The modern power system is experiencing an unprecedented evolution. On the one hand, large-scale interconnected power systems have emerged in some countries. On the other hand, the installed renewable energy capacity, especially the wind power, has been increasing rapidly to satisfy the growing power demand and the desire for sustainable development.

With the interconnection of large regional grids, tie-line power oscillations happen more frequently than before, which can limit the transmission capacity or even jeopardize the system stability. For instance, in Finland-Sweden-Norway-Denmark system and Western Electric Coordinating Council system (WECC), tie-line power oscillations have resulted in the separation of the interconnected system on some occasions [1]. Normally, tie-line power oscillations are associated with inter-area oscillations which involve two coherent groups of generators swinging against each other. This type of oscillation corresponds to a low frequency oscillation which frequency is in the range of 0.1–2.5 Hz [2].

Previous work has pointed out that cyclic external disturbances can result in a significant response in power systems, when their fundamental frequency is close to the low-frequency oscillation mode (including inter-area mode) of the system [3,4]. These kinds of oscillations are termed forced oscillations. In the past, the forced oscillations didn't arouse much attention, as they showed little impact on power system stability. However, in recent years, forced oscillation accidents induced by small hydro plants have happened several times in the China Southern Power Grid, which is a typical interconnected grid with low damping inter-area modes [5]. Hence, attention to forced oscillations has been renewed.

Wind power variations can also be considered as an external disturbance to power systems. Power variations produced by wind turbines during continuous operation are mainly caused by wind speed variations, tower shadow effects, wind shear effects, *etc*. The effects of tower shadow and wind shear (TSWS) produce a periodic reduction in mechanical torque at a frequency called the 3p frequency [6]. The 3p frequency range, due to rotational sampling as each blade passes the tower, tends to coincide with the frequency range associated with inter-area oscillations, so the power variations induced by TSWS might be a source of forced oscillations that can excite system resonance.

The TSWS are referred to as 3p oscillations. The 3p oscillations once aroused great attention from the power quality point of view, as researchers have found that 3p oscillations are one of the main contributors to flicker emissions produced by wind farms. Compared with fixed-speed wind turbines, variable-speed wind turbines have shown better performance in flicker emission [7]. Subsequently, several active or reactive power control methods have been proposed to eliminate flicker, especially for variable-speed wind farms [7–9]. However, the effects of power variations due to TSWS are not taken into account in the assessments of power system stability assuming that the mechanical torque for the wind turbine is constant [10]. That is to say, comprehensive understanding of the adverse effects of 3p oscillation is still limited, and it is necessary to reevaluate this phenomenon.

Recently, the power system oscillations induced by TSWS have been discussed. Brownlees *et al*. [11] have investigated the impact of TSWS from fixed-speed wind farm power oscillations on the Irish Power System based on recorded data analysis. Hu *et al.* [12] have simulated that the TSWS of a wind farm can induce tie-line power oscillations. However, the above results are preliminary and cannot readily offer qualitative conclusions, so the underlying mechanism needs to be studied further.

Besides, it is also important to quantify the magnitude of tie-line power oscillations induced by 3p oscillations and to study the qualitative effects of parameters.

With the aim of evaluating the impact of TSWS on tie-line power oscillations, this paper addresses the issue of integration of a large-scale wind farm into interconnected power systems. In Sections 2–4, the transfer functions of a wind farm, a simplified two-zone system and a combined system are developed, respectively. Frequency domain analysis is used to identify potentially amplified-response conditions, the worst case and qualitative parametric effects. In Sections 5 and 6, time-domain simulations are subsequently applied in the two-area four-generator test system and the more realistic WECC 127 bus system to accurately quantify the effect in the worst case. A new horizon is provided to see how and when the TSWS affect power systems stability.

2. Disturbance Source Modeling

Wind turbine models for power system studies have been widely discussed. The fixed-speed wind turbine models mainly include the aerodynamics model, the shaft model, the generator model and pitch control. With the development of wind turbines, the technology has switched from fixed to variable speed. The variable-speed wind turbine models include more models like the converters model and their controller model.

Since the phenomenon of inter-area oscillations is the topic of interest, a simplified wind turbine and system models in the frequency domain are proposed, which only consider the dynamic model in the low frequency oscillations range. However, the complete models of the wind turbine and power systems are adopted in the simulation study to verify the results.

2.1. Aerodynamics Model

Because the electrical behavior of wind turbines is the main topic of interest of the study, a simplified aerodynamic model [13] is used as follows:

$$T_{\mathrm{m}} = 0.5\rho\pi R^3 \frac{C_p(\lambda,\theta)}{\lambda} V_{\mathrm{eq}}{}^2 \tag{1}$$

where T_{m} is the mechanical torque, ρ is the air density, R is the wind turbine rotor radius, V_{eq} is the equivalent wind speed, C_p is the aerodynamic efficiency of rotor, λ is the tip speed ratio and θ is the pitch angle of the rotor.

Most studies concerning the stability of power systems with integrated wind power generally neglect the 3p oscillations. Here, a comprehensive model of 3p mechanical torque for a three-blade wind turbine [6] is adopted. Based on this model, the equivalent wind speed can be expressed by three components, as follows:

$$V_{\mathrm{eq}} = V_{\mathrm{H}} + V_{\mathrm{eqws}} + V_{\mathrm{eqts}} \tag{2}$$

where V_{H} is the wind speed at hub height, V_{eqws} is the wind shear component, V_{eqts} is the tower shadow component. The latter two components can be represented as:

$$V_{\mathrm{eqws}} = V_{\mathrm{H}}[\frac{\alpha(\alpha-1)}{8}(\frac{R}{H})^2 + \frac{\alpha(\alpha-1)(\alpha-2)}{60}(\frac{R}{H})^3 \cos 3\beta] \tag{3}$$

$$V_{\text{eqts}} = \frac{mV_{\text{H}}}{3R^2}\sum_{b=1}^{3}\left[\frac{a^2}{\sin^2\beta_b}\ln\left(\frac{R^2\sin^2\beta_b}{x^2}+1\right)-\frac{2a^2R^2}{R^2\sin^2\beta_b+x^2}\right] \quad (4)$$

where α is the empirical wind shear exponent, H is the elevation of rotor hub (m), β is the azimuthal angle of the blade (deg), β_b is the azimuthal angle of each blade (deg), a is the tower radius (m), x is the distance from the blade origin to the tower midline (m), and $m = 1 + [\alpha(\alpha - 1)]/8 \times (R/H)^2$ is a coefficient of the wind turbine.

Linearizing Equation (1) and substituting for V_{eq} given by Equation (2), it indicates that mechanical torque variations induced by TSWS are also periodic and the magnitude of 3p oscillations varies with different mechanical and operation parameters of wind turbines.

The 3p frequency ($f_{3\text{p}}$) is three times of rotor frequency. For different fixed-speed wind turbines, typically, $f_{3\text{p}}$ can be in the range of 0.65 Hz to 1.5 Hz, which is calculated from some typical parameters provided by Siemens and Vestas (Aarhus, Denmark) [11,13], and the magnitude of 3p oscillations power is about 10% of the average power output.

For a variable-speed wind turbine, the $f_{3\text{p}}$ of the popular variable-speed wind turbines varies from 0.25 to 0.9 Hz which is calculated from some typical parameters provided by General Electric Co. (GE, Fairfield, CT, USA) and Siemens Wind Power A/S (Brande, Denmark) [13,14]. Taking a GE 2.7 MW variable-speed wind turbine and Siemens 1.3 MW fixed-speed wind turbine as examples, we plot the 3p frequency under different wind speeds, as shown in Figure 1.

Figure 1. 3p Frequency with two types of wind turbine.

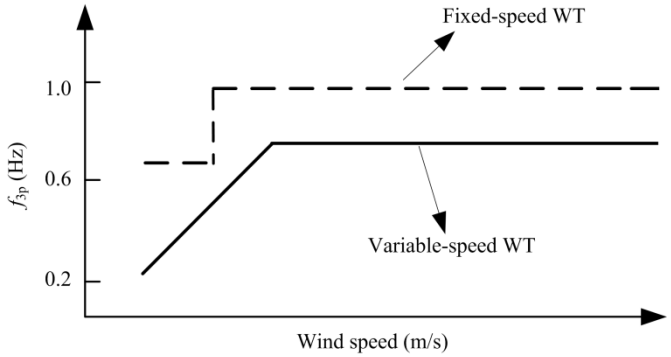

Figure 1 shows that the $f_{3\text{p}}$ is in the range of interest of low frequency oscillations. This fixed-speed wind turbine has two 3p frequencies for a switch between the two windings and it is easy to form a sustainable oscillations source. When a variable-speed wind turbine operates at its maximum power point tracking (MPPT) range, the $f_{3\text{p}}$ is proportional to the wind speed, while the wind speed is above the rated wind speed, the $f_{3\text{p}}$ is constant. When the variable-speed wind turbine operates around a fixed wind speed or at mid-high wind speed, the variable-speed wind turbine can also form a forced oscillations source.

2.2. Shaft Model

The wind turbine system has a low resonant frequency due to the softness of the low speed shaft. Thus the dynamics of the shaft model need to be taken into account. The two-mass model

representation of the shaft is proper to illustrate the dynamic impact of wind turbines on low frequency oscillations in grids. The linearized form of the shaft two-mass model [13] is:

$$\begin{cases} 2H_{\mathrm{W}}\dfrac{d\Delta\omega_1}{dt} = \Delta P_{\mathrm{m}} - K_{12}\Delta\theta - D_{12}(\Delta\omega_1 - \Delta\omega_2) \\ 2H_{\mathrm{G}}\dfrac{d\Delta\omega_2}{dt} = K_{12}(\Delta\theta) + D_{12}(\Delta\omega_1 - \Delta\omega_2) - \Delta P_{\mathrm{e}} \\ \dfrac{d\Delta\theta}{dt} = \omega_0(\Delta\omega_1 - \Delta\omega_2) \end{cases} \tag{5}$$

where P_{e} is the electric power of the generator, P_{m} is the mechanical power produced by rotating wind turbine, ω_1, ω_2 are the speeds of the wind turbine and the generator rotor, ω_0 is the rated grid speed, θ *i*s the twist angle in the shaft system, K_{12} is the shaft stiffness, D_{12} is the damping coefficient between wind turbine and generator, H_{W} and H_{G} are inertia constants of the wind turbine and generator, the prefix Δ denotes a small deviation.

By taking the Laplace transform of Equation (5), the equations can be written in the frequency domain with the initial conditions of state variable deviations assumed to be zero as:

$$\begin{cases} 2H_w s\Delta\omega_1(s) = \Delta P_m(s) - K_{12}\Delta\theta(s) - D_{12}[\Delta\omega_1(s) - \Delta\omega_2(s)] \\ 2H_G s\Delta\omega_2(s) = K_{12}\Delta\theta(s) + D_{12}[\Delta\omega_1(s) - \Delta\omega_2(s)] - \Delta P_e(s) \\ s\Delta\theta(s) = \omega_0[\Delta\omega_1(s) - \Delta\omega_2(s)] \end{cases} \tag{6}$$

Since the wind turbine is operating in the speed control mode, $\Delta\omega_2$ can be assumed to be zero. The response of electrical power can be derived from Equation (6), as follows:

$$\Delta P_{\mathrm{e}} = \frac{\omega_0 K_{12} + D_{12}s}{\omega_0 K_{12} + D_{12}s + 2H_{\mathrm{W}}s^2}\Delta P_{\mathrm{m}} \tag{7}$$

2.3. Generator Model, Converter Model and Control Strategies

For convenience, a variable-speed wind turbine based on a multi-pole permanent magnet synchronous generator (PMSG) [15] is applied here as an example. We should note that in this study the PMSG only adopts basic control without ancillary controllers to eliminate the 3p oscillations. Neglecting the stator transient, the equations of a PMSG can be expressed by a set of algebraic equations [2].

For the converters, the switch frequency of the power electronic components far exceeds the frequency band of interest, so an average model is used without considering switch dynamics [16].

Normally, variable-speed wind turbines have two control goals, depending on the wind speed. At low-moderate wind speeds, the rotor speed can be adjusted with the wind speed so that the optimal tip speed ratio is maintained for maximum power point tracking (speed control mode). At high wind speeds, the wind turbine maintains the rated output power by adjusting the pitch angle and keeping the rotor speed constant (power limitation mode). The vector-control is used to realize the decoupled control of active power and reactive power. The control strategies used in this study are based on the idea [15] that the generator-side converter controls the rotor speed to maintain the optimal tip speed ratio and minimize the power losses in the generator, while the grid-side converter control DC-link voltage constant and reactive power flow to the grid. More details on the controller model are given by

Chinchilla *et al*. [15]. In the time scale of electromechanical dynamic, the power loss of power electronic converter can be ignored. Hence, the output power fluctuation of a wind turbine ΔP_{WT} approximately equals to ΔP_{e}.

2.4. Wind Farm Model

The fluctuation power of a wind farm which consists of N wind turbines can be expressed as:

$$\Delta P_{WF} = \alpha_1 \sum_{i=1}^{N} \Delta P_{WT_i} = \alpha_1 \frac{\omega_0 K_{12} + D_{12} s}{\omega_0 K_{12} + D_{12} s + 2 H_w s^2} \Delta P_{mN} \tag{8}$$

where α_1 is the TSWS weaken factor ($0 < \alpha_1 < 1$), i is the number of wind turbines, and $\Delta P_{\mathrm{m}N}$ is the sum of the mechanical power fluctuation of N wind turbines.

Normally, for every wind turbine in a wind farm, the time of a blade passing by the tower is stochastic. The power drop time depends on not only the rotor speed, but also the initial phase. This means that a wind farm's power fluctuation induced by TSWS will be weakened due to the random blade position. When $\alpha_1 = 0$, it represents that the TSWS can be totally cancelled out if the turbines could be controlled to distribute the rotor angle evenly. When $\alpha_1 = 1$, it represents that the blades are synchronized and the blades are passing by the tower at the same time, thus the superposition of the 3p oscillations will cause the maximum power fluctuation ($N\Delta \mathrm{P_{WT}}$). It should be noted that, the case of $\alpha_1 = 1$ is not expected to represent a typical operation but rather to be a representative of "the worst case". Since we try to figure out the worst impact of the TSWS on power systems, we choose the case of $\alpha_1 = 1$ for the following study. With per unit expression, $\Delta P_{\mathrm{m}N} = \Delta P_{\mathrm{m}}$, then the transfer function representing the relationship between mechanical power fluctuation and output power fluctuation of the wind farm can be expressed as:

$$G_1(s) = \frac{\Delta P_{\mathrm{WF}}}{\Delta P_{\mathrm{m}}} = \alpha_1 \frac{\omega_0 K_{12} + D_{12} s}{\omega_0 K_{12} + D_{12} s + 2 H_{\mathrm{W}} s^2} \tag{9}$$

According to Equation (9), the frequency characteristic of the wind turbine system shows that the wind turbine acts like a low pass filter and when the mechanical power disturbance is constant, the wind power variation of a wind farm is linear to the TSWS weaken factor α_1. Based on some typical parameters of a wind turbine [13], the natural resonant frequency of the wind turbine ($f_{1\mathrm{n}}$) is in the range of 0.11 to 0.82 Hz which means that the 3p oscillations are likely to be amplified in the wind turbine. Besides, it is notable that the operation point of the wind turbine has no effect on its natural frequency.

3. Tie-Line Power Oscillations Induced by a Wind Farm

3.1. Modeling of Tie-Line Power Oscillations

For a typical two-area interconnected power system, the closely coupled generators in each zone can be equivalent to one generator. Therefore, in order to focus on how power variations of a wind farm affect the tie-line power, a simple two-machine system with a wind farm is constructed. The configuration is shown in Figure 2. The system consists of two similar generators (Gen 1 and Gen 2) and a wind turbine which is connected to Bus 1. Analysis of a system with such a simple configuration is useful in understanding the fundamental of tie-line power oscillations and studying the parametric effects.

Figure 2. A two-machine system with a wind farm.

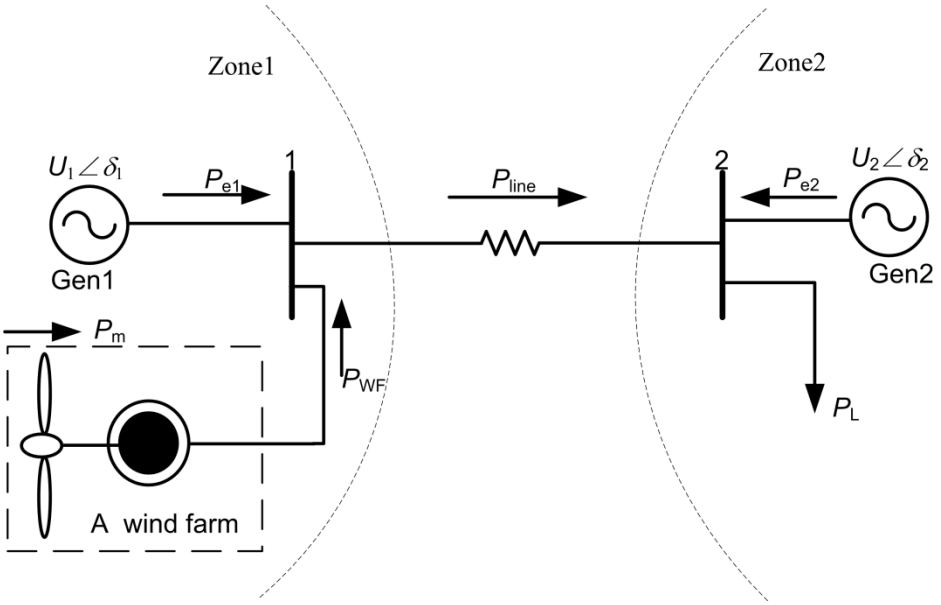

With the synchronous generator represented by a classical model [2], the linearized swing equations of Gen1 and Gen2 are given by:

$$\begin{cases} \dfrac{2H_1}{\omega_0}\dfrac{d^2\Delta\delta_1}{dt^2}+\dfrac{K_{D1}}{\omega_0}\dfrac{d\Delta\delta_1}{dt}=\Delta P_{m1}-\Delta P_{e1} \\ \dfrac{2H_2}{\omega_0}\dfrac{d^2\Delta\delta_2}{dt^2}+\dfrac{K_{D2}}{\omega_0}\dfrac{d\Delta\delta_2}{dt}=\Delta P_{m2}-\Delta P_{e2} \end{cases} \tag{10}$$

where H_1, H_2, δ_1, δ_2, K_{D1}, K_{D2} are the inertia constants, the rotor angles, the damping coefficients of Gen1 and Gen2, respectively; P_{m1}, P_{m2}, P_{e1}, P_{e2} are the mechanical power and the electrical power of Gen1 and Gen2.

According to the power conservation principle with assuming the tie-line is lossless, we obtain:

$$\begin{cases} \Delta P_{e1}=\Delta P_{\text{line}}-\Delta P_{\text{WF}} \\ \Delta P_{e2}=-\Delta P_{\text{line}}+\Delta P_{\text{L}} \end{cases} \tag{11}$$

where P_{WF}, P_{line}, P_L are the active power of the wind farm, the tie-line and the load.

Here ΔP_{line} can be expressed as:

$$\Delta P_{\text{line}}=\frac{U_1U_2\cos\delta_{120}}{x_{12}}\Delta\delta_{12} \tag{12}$$

where x_{12} is the reactance of the tie-line, δ_{120} and $\Delta\delta_{12}$ are the initial angle difference and the angle difference deviation between Gen1 and Gen 2. U_1 and U_2 are the terminal voltages.

Assuming that $\Delta P_{m1} = \Delta P_{m2} = 0$, $\Delta P_L = 0$, for convenience, the model adopts equivalent damping [17], by defining $K_{D1}/2H_1 = K_{D2}/2H_2 = K_D$. Combining Equation (11) with Equation (10) and substituting for $\Delta\delta_{12}$ by Equation (12) and we have:

$$\frac{d^2\Delta P_{\text{line}}}{dt^2}+K_{\text{D}}\frac{d\Delta P_{\text{line}}}{dt}+K_{\text{s}}\Delta P_{\text{line}}=\frac{\omega_0}{2H_1}\frac{U_1U_2\cos\delta_{120}}{x_{12}}\Delta P_{\text{WF}} \tag{13}$$

where $K_s = \frac{\omega_0}{2}(\frac{1}{H_1}+\frac{1}{H_2})\frac{U_1U_2\cos\delta_{120}}{x_{12}}$.

By defining $\alpha_2 = \frac{\omega_0}{2H_1}\frac{U_1U_2\cos\delta_{120}}{x_{12}}$, which can be treated as the contribution factor of the wind farm power variations, and taking the Laplace transform of Equation (13), the transfer function representing the relationship between the wind farm power variations and the tie-line power oscillations can be expressed as:

$$G_2(s) = \frac{\Delta P_{\text{line}}}{\Delta P_{\text{WF}}} = \frac{\alpha_2}{s^2 + K_{\text{D}}s + K_{\text{s}}} \tag{14}$$

According to Equation (14), the frequency response characteristic is not only dependent on the system parameters, but also the initial operation point which is associated with δ_{120}, U_1 and U_2. In general, system natural frequency ($f_{2\text{n}}$) is in the low frequency oscillation range of 0.1 to 2.5 Hz in interconnected systems.

3.2. Frequency Response Analysis

Frequency response characteristic illustrates the severity of the disturbance under different frequencies. A numerical example based on typical parameters [2] is used to demonstrate the tie-line frequency response characteristic. The values of the system parameters are as follows: H_1 = 6.5 s, H_2 = 6.175 s, K_{D1} = 5, $U_1 = U_2$ = 1.01 p.u., δ_{120} = 0.4 rad, x_{12} = 1 p.u. Based on above parameters, the amplitude-frequency response characteristic of $G_2(\text{j}\omega)$ is plotted in Figure 3.

Figure 3. Amplitude-frequency response characteristic of $G_2(\text{j}\omega)$.

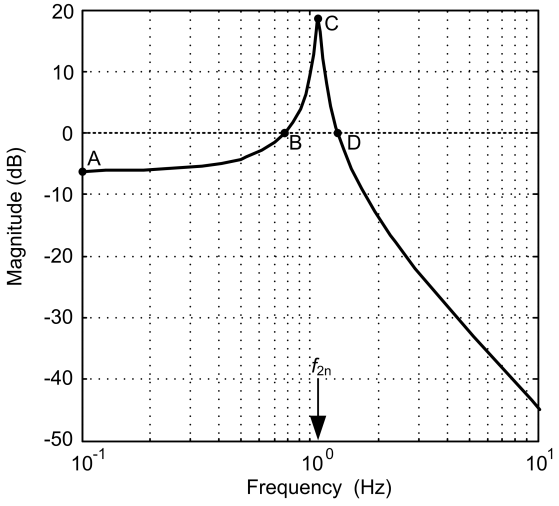

When $f_{3\text{p}} \in$ [A,B], $|G_2(\text{j}\omega)| < 1$. Namely, the tie-line power oscillation is less than the power fluctuation of a wind farm (A: $|G_2(\text{j}\omega)| = 0.51$, B: $|G_2(\text{j}\omega)| = 1$), which means that the synchronous generators dampen the disturbance of the wind farm in AB. When $f_{3\text{p}} \in$ [D,∞), $|G_2(\text{j}\omega)| < 1$ and attenuates very fast, which means that the two-machine system acts as a low-pass filter and thus the high-frequency disturbance from a wind farm has little effect on the tie-line power (D: $|G_2(\text{j}\omega)| = 1$). When $f_{3\text{p}} \in$ (B,D), $|G_2(\text{j}\omega)| \geq 1$. Namely, the amplitude of the tie-line power oscillation is larger than the power fluctuation of a wind farm. Especially, when $f_{3\text{p}}$ closes to the system natural frequency $f_{2\text{n}}$

(C: $|G_2(j\omega)|_{max} = 8.71$, $f_{2n} = 1.09$ Hz), the tie-line power oscillations will be sharply amplified, which is caused by resonance.

3.3. The Expression of the Peak Magnitude

The occurrence of resonance is a severe disturbance to power systems. Therefore, it is essential to evaluate the peak magnitude of the tie-line power resonance. Define the damping ratio $\zeta = K_D / 2\sqrt{K_s}$ and let $\omega_{2n} = 2\pi f_{2n} = \sqrt{K_s}$, thus $G_2(s)$ can be rewritten as a standard form as follows:

$$G_2(j\omega) = \frac{\alpha_2 / K_s}{(j\frac{\omega}{\omega_{2n}})^2 + j2\zeta\frac{\omega}{\omega_{2n}} + 1} \tag{15}$$

Let the derivative of Equation (15) with respect to ω/ω_{2n} equal to be zero and the expression of the system resonant frequency ω_r is:

$$\omega_r = \omega_{2n}\sqrt{1-2\zeta^2} \tag{16}$$

Normally, the typical damping ratio of inter-area mode in power systems is close to zero [2], so ω_r is close to ω_{2n} according to Equation (16). Consequently, when f_{3p} approaches the system natural frequency f_{2n}, the resonant peak magnitude of the tie-line power oscillations is given by:

$$|\Delta P_{line}| = |G_2(j\omega)|_{max} \cdot |\Delta P_{WF}| = \frac{1}{H_1/H_2 + 1}\cdot\frac{1}{2\zeta}\cdot|\Delta P_{WF}| \tag{17}$$

3.4. Parametric Analysis

Equation (17) illustrates that the resonant magnitude of the tie-line power oscillation is dependent on three factors: the disturbance magnitude of the wind farm (ΔP_{WF}), the inertia constant ratio of two-area systems (H_1/H_2) and the system damping ratio (ζ). As ΔP_{WF} increases, or H_1/H_2 deceases, or ζ decreases, the peak magnitude of the tie-line power oscillations increases. $H_1/H_2 > 1$ means that the wind farm connects to a relatively big grid, $H_1/H_2 < 1$ means that the wind farm connects to a relatively small grid and $H_1 = H_2$ means that the wind farm connects to a grid with two identical areas.

As shown in Table 1, the numerical examples are given to calculate $|G_2(j\omega)|_{max}$ with three different inertia constant ratios, *i.e.*, 1/25, 1/1, and 25/1, denoted by Case 1 Case2 and Case3. In each case, there are three damping ratios, *i.e.*, 0.3, 0.05 and 0.01, corresponding to the good, medium and poor damping, respectively.

Table 1. $|G_2(j\omega)|_{max}$ with different inertia constant ratios and damping ratios.

Case	H_1/H_2	$\|G_2(j\omega)\|_{max}$		
		$\zeta = 0.3$	**$\zeta = 0.05$**	**$\zeta = 0.01$**
1	1/25	1.60	9.62	48.08
2	1/1	0.83	5	25
3	25/1	0.06	0.38	1.92

Table 1 shows that with "big" grid connections (e.g., Case 3) the wind farm has limited influence on the tie-line power fluctuations. When the resonance happens in a medium damping system (ζ = 0.05), the tie-line power oscillations induced by TSWS can be neglected since $|\Delta P_{line}|$ is less than half of $|\Delta P_{WF}|$.

However, when the wind farm is integrated into a "small" grid (e.g., Case 1), even with a good damping system (ζ = 0.3), $|\Delta P_{line}|$ is 1.6 times higher than $|\Delta P_{WF}|$. Furthermore, with a poor damping of the tie-line mode, $|\Delta P_{line}|$ is 48.08 times higher than $|\Delta P_{WF}|$. Thus attention must be paid to the risk of the tie-line power oscillations.

In some countries, such as China, the wind sources may be far away from the load centers. Because it is hard to accommodate all the wind power in the local grid, the residual wind power has to be transferred to a distant load center through long transmission lines, e.g., the wind power in Gansu Jiuquan is a practical case [18]. This is similar with Case1. Thus the risk of the tie-line power oscillations induced by TSWS is worthy of discussion.

4. Combination of the Wind Turbine System and Power Systems

According to Figure 2, the tie-line power oscillations induced by 3p oscillations can be described by the form of two subsystems series in Figure 4. The overall frequency response of the cascade of two subsystems is the product of the individual frequency response.

Figure 4. Block diagram of the series interconnection of the two subsystems.

Combining Equation (9) with Equation (14), the transfer function of representing the relationship between ΔP_m and ΔP_{line} can be expressed as:

$$G_3(s) = \Delta P_{line} / \Delta P_m = G_1(s) \cdot G_2(s) = \frac{\alpha_1(\omega_0 K_{12} + D_{12}s)}{\omega_0 K_{12} + D_{12}s + 2H_W s^2} \cdot \frac{\alpha_2}{s^2 + K_D s + K_s} \quad (18)$$

For analyzing the combined impact of these two subsystems, two sets of typical parameters are used in the following example. For the wind turbine system, H_w = 4.54 s, K_{12} = 0.5 p.u./el.rad, D_{12} = 7.5 p.u./el.rad. For the two-machine system, the values of the parameters are the same as those in Section 3.2. For power systems, G_1(s) is normally fixed due to the unchangeable mechanical characteristics of the wind turbine, whereas G_2(s) continuously changes with different system operation conditions or power flows.

The amplitude-frequency characteristics of $G_1(j\omega)$, $G_2(j\omega)$ and $G_3(j\omega)$ are calculated based on the aforementioned parameters, as shown in Figure 5, where the two panels correspond to two different cases: (A) $G_1(j\omega)$ and $G_2(j\omega)$ have different natural frequencies, *i.e.*, $f_{1n} \neq f_{2n}$, (B) $G_1(j\omega)$ and $G_2(j\omega)$ have equal natural frequencies, *i.e.*, $f_{1n} \approx f_{2n}$. Figures 5A,B has same $G_1(j\omega)$, but different $G_2(j\omega)$ by changing the reactance of the tie-line. In the plots, each peak is an indication of a resonant frequency in systems. A relatively large response can be achieved, when f_{3p} approaches the resonant frequency (f_{1n} or f_{2n}).

Figure 5. Amplitude-frequency characteristic of $G_1(s)$, $G_2(s)$ and $G_3(s)$. (**A**) $f_{1n} \neq f_{2n}$; (**B**) $f_{1n} \approx f_{2n}$.

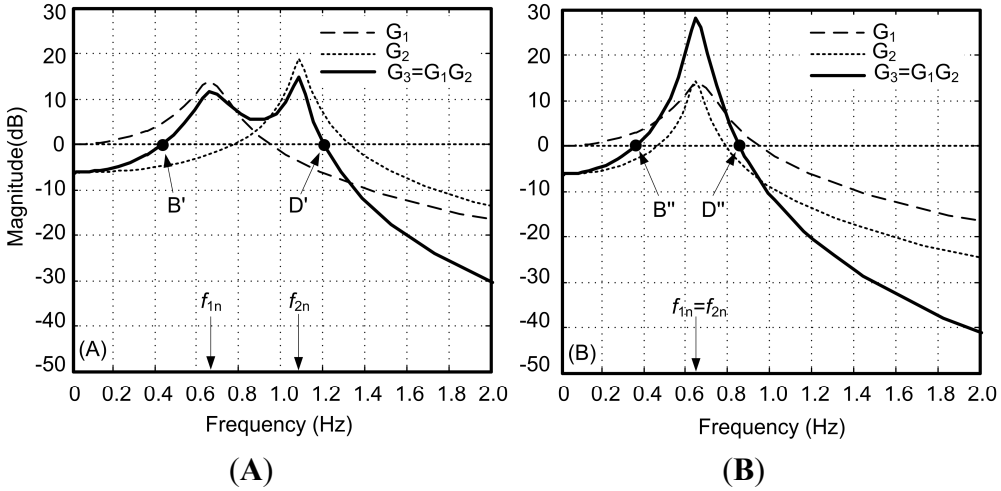

(A) **(B)**

Figure 5A illustrates that when the wind turbine systems are integrated into a two-machine system, another new peak is created in the low frequency range (f_{1n} = 0.66 Hz), which was not reported in previous studies. Because the natural frequency of the soft shaft of the wind turbine is within the low frequency oscillation range and thus it may be able to interact with the electromechanical performance of power systems. The plot of $|G_3(j\omega)|$ shows that the amplified frequency range is from 0.44 to 1.21 Hz (B'D') which is hardly obtained from eigenvalue analysis. Two peaks appear at f_{1n} = 0.66 Hz, f_{2n} = 1.09 Hz, respectively. Due to the interaction of $G_1(j\omega)$ and $G_2(j\omega)$, $|G_3(j\omega)|_{max}$ equals to 5.3 which is less than any peak of $G_1(j\omega)$ and $G_2(j\omega)$.

Figure 5B indicates that $|G_3(j\omega)|$ only has one peak when f_{2n} approaches f_{1n} (0.66 Hz). The amplified magnitude is the production of the amplifications of two subsystems. $|G_3(j\omega)|_{max}$ equals to 26.6, which is much larger than the peak magnitude of any subsystem. That means the most serious situation may arise in interconnected systems, especially when the system natural oscillation frequency (f_{2n}) approaches the newly created peak (f_{1n}). The amplified frequency range is from 0.36 to 0.85 Hz (B''D''). Compared with Figure 5A, $|G_3(j\omega)|$ increases more sharply, though the amplified frequency range reduces slightly.

Moreover, the f_{3p} has a large chance to appear in the amplified range. Taking the typical parameters in Section 2.4 as examples, the range of f_{3p} is about 0.25–0.90 Hz. This means that when the wind turbine operates at middle or high wind speed, $|G_3(j\omega)|$ is larger than 1. Especially when the wind speed is over the rated wind speed, f_{3p} will be fixed that increases the opportunities to be a continuous periodic source. Nowadays, with the development of low-speed large-capacity wind turbine technology, the maximum rotor speed of a wind turbine becomes lower and lower. This trend will increase the risk of resonance.

The theoretical analysis above is based on a simplified two-machine system. The prediction of this model is pessimistic, since the transfer function given by Equation (18) ignores excitation control and other controllers which may affect the system damping. For a multi-machine system, the damping factors and the electrical components are more complicated and coupled. However, the above frequency domain analysis, which gives more details than eigenvalue analysis, is still useful for understanding the principle and analyzing influence factors qualitatively. The general conclusions drawn from the theoretical work will be confirmed by a test system and a more realistic large system.

5. Case I: Modified Two-Area Four-Generator System

5.1. System Description

The modified test system is realized by adding an aggregated PMSG-based wind farm to the two-area system four-generator which is widely used to study the fundamental of inter-area oscillations [19]. The structure of the system is shown in Figure 6.

Figure 6. A modified two-area four-generator system with a PMSG-based wind farm.

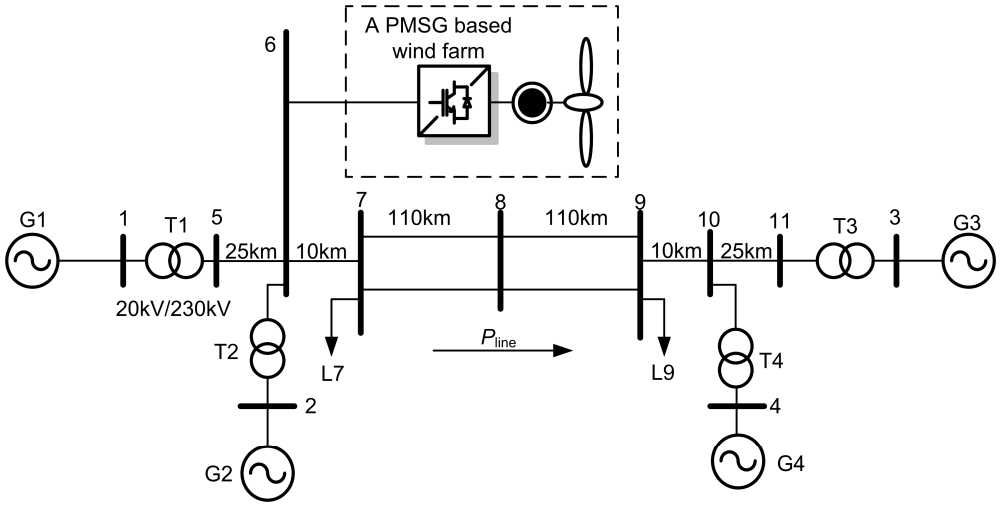

The base system consists of two similar areas connected through a tie-line. Each area consists of two synchronous generating units, having a rating of 900 MW. The synchronous generator model includes the excitation system and the governor but no power system stabilizer. The loads are represented as constant impedance loads at Bus 7 and Bus 9. The parameters of generators, lines and load are given in the Appendix, and more details can be found in Kundur's book [2]. The wind farm, which consists of 100 wind turbines (each with a capacity of 2 MW), connects to Bus 6. The wind turbine model consists of the aerodynamic model considering TSWS, the two-mass shaft model, the PMSG, the converter model and the control systems. The parameters of wind turbines are given in appendix [16]. All above simulation models are developed in a power system analysis tool PSCAD/EMTDC. The system operates with Area 1 exporting 400 MW to Area 2.

In order to get the inter-area modes, a small disturbance is imposed to excite the inter-area oscillations and the time-domain response of tie-line power is recorded. The total least square estimation of signal parameters via rotational invariance techniques (TLS-ESPRIT) method [20], which is a signal processing method of proving efficient and good noise immunity in mode identification, is used to identify the dominant inter-area mode. In addition, the parameters of the original system is adjusted to make the frequency of the inter-area mode (f_{2n}) approaching the wind turbine natural oscillation frequency (f_{1n} = 0.66 Hz) thus to simulate the worst case.

5.2. Simulation Results

5.2.1. Effects of the Wind Speed

The wind generator frequently changes its operating points as the wind speed fluctuates. The operation point of a wind turbine is an important factor to decide f_{3p} and $|\Delta P_m|$. To test the effect of the 3p oscillations on the tie-line power oscillations at different wind speeds, fourteen operating conditions, including wind speeds from 5 m/s to 11.5 m/s with a 0.5 m/s step, are considered. The Fast Fourier Transform (FFT) method is used to analyze their spectrums. Figure 7A shows the plots of the tie-line power oscillations as a function of time for three wind speeds: 7.5, 8.5 and 9.5 m/s. Figure 7B shows their corresponding spectrum analysis.

Figure 7. Tie-line power oscillations and spectrum analysis with three wind speeds: (**A**) Variation of the tie-line active power; (**B**) Spectrum analysis.

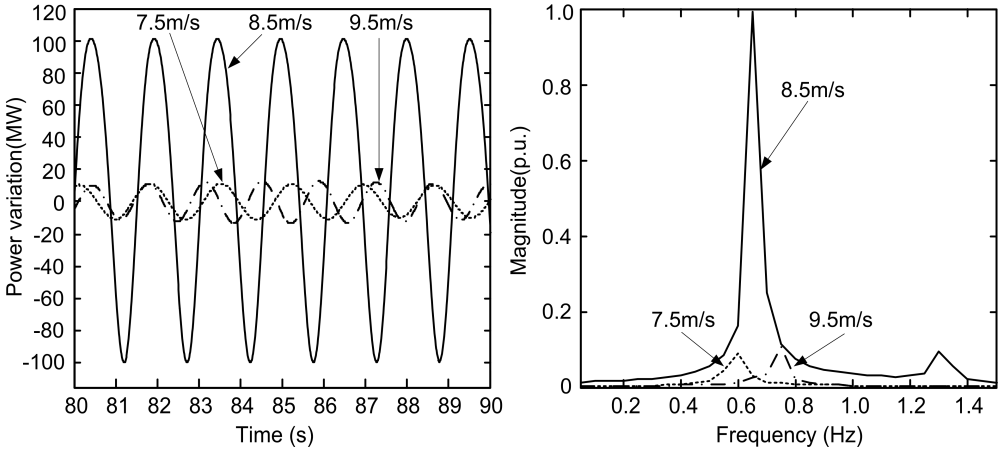

(A) **(B)**

Figure 7A shows that the magnitude of tie-line power oscillations at wind speed 8.5 m/s is much greater than the other two wind speeds. The magnitude of tie-line power oscillations reaches 100 MW (nearly 25% of the transmission rated capacity), which increases the risk of power system operation. Figure 7B shows that when the wind speeds equal 7.5, 8.5 and 9.5 m/s, f_{3p} are 0.58, 0.66 and 0.73 Hz, respectively. That means the large tie-line power oscillation is caused by the resonance when f_{3p} closes to 0.66 Hz (f_{2n}).

To illuminate the impact of different operation points on tie-line power oscillations quantitatively, three amplification factors are defined as follows: $\beta_1 = |\Delta P_{WF}|/|\Delta P_m|$, $\beta_2 = |\Delta P_{line}|/|\Delta P_{WF}|$, $\beta_3 = |\Delta P_{line}|/|\Delta P_m|$. With measuring f_{3p}, $|\Delta P_m|$, $|\Delta P_{WF}|$ and $|\Delta P_{line}|$, respectively, and a set of f_{3p} and amplification factors with different wind speeds can be calculated. Figure 8 illustrates 3p frequency (Figure 8A) and amplification factors β_1, β_2 and β_3 (Figure 8B) as a function of wind speed.

As shown in Figure 8A, when wind turbines operate in the maximum power point tracking range (5–10 m/s), f_{3p} increases with the increase of the wind speed; when the rotor speed reaches the maximum value (10–11.5 m/s), f_{3p} keeps constant. When wind speed equals to 8.5 m/s, f_{3p} is 0.66 Hz which closes to f_{2n} and f_{1n}.

Figure 8B indicates that $2 < \beta_1 < 5$ in the overall tested wind speed range, where the soft shaft can amplify the mechanical power fluctuation. Differently, $\beta_2 > 1$ only when the wind speed is in the range of 7–9 m/s, and $\beta_2 < 1$ in the rest of the wind speed range. Similarly, $\beta_3 > 1$ when the wind speed is in the range of 5.5 to 10 m/s. Especially, when wind speed equals to 8.5 m/s, β_3 equals to 25, which means that the original mechanical variations has been amplified for 25 times. The simulation results agree with the theoretical analysis in Figure 5B.

Figure 8. f_{3p} (**A**) and amplification factors (**B**) as a function of wind speeds.

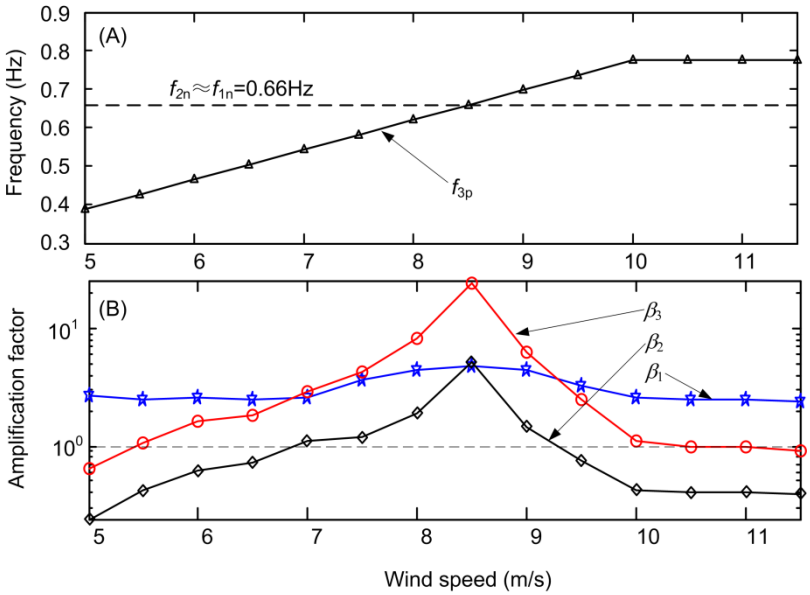

The above simulations relay on the premise that the TSWS weaken factor $\alpha_1 = 1$. According to Equation (18), the magnitude of tie-line power oscillations is also linear to α_1. This means that even when $\alpha_1 = 0.5$ or 0.2, the magnitude of tie-line power oscillations will be 50 or 20 MW, approximately, when the wind speed is equal to 8.5 m/s. Thus this phenomenon should still be noticed in power systems, since it will reduce the transmission capacity and harm the system operation.

5.2.2. Effects of System Parameters

To validate the predication of qualitative parametric analysis in Section 3.4, different system inertia ratios, wind farm penetration capacities and tie-line impedances are adopted in the simulations. Figure 9 shows the results under the resonant conditions.

(A) Effect of the Integrated System Inertia

The nature characteristic of an AC system and the associated problems are highly dependent on the inertia of the AC system. The time domain simulations were carried out to validate the impact of the integrated system inertia on tie-line power oscillations. Four conditions are considered in these tests: keep the inertia of the sending system connected with a wind farm as $H_1 = 5.25$ and changing the receiving system inertia as $H_2 = 2.925$, 4.925, 8.925 and 14.925, respectively. According to Section 3.3, f_{2n} changes with the H_2. In these tests, keep the tie-line power flow and variations of the wind farm output power unchanged, and set the disturbance frequency f_{3p} approaching f_{2n}.

Figure 9A shows that the resonant frequency is highest for H_2 = 2.925 and lowest for H_2 = 14.925 and the magnitude is highest for H_2 = 14.925 and lowest for H_2 = 2.925. The curves illuminate that while inertia ratio H_1/H_2 decreases, f_{2n} decreases and the magnitude of tie-line power oscillations increases. The above analysis implies that when the wind farm connects to a subsystem with a relatively low inertia, the variations of wind farm output power may increase the risk of the tie-line power oscillations and when the wind farm connects to a subsystem with a relatively high inertia, the fluctuation of wind farm output power has a less contribution to tie-line power oscillations, even in a resonant case. These results are well consistent with the findings in Section 3.4.

Figure 9. Tie-line power oscillations with (**A**) different inertias of integrated subsystem; (**B**) different capacities of wind farm; (**C**) different tie-line lengths.

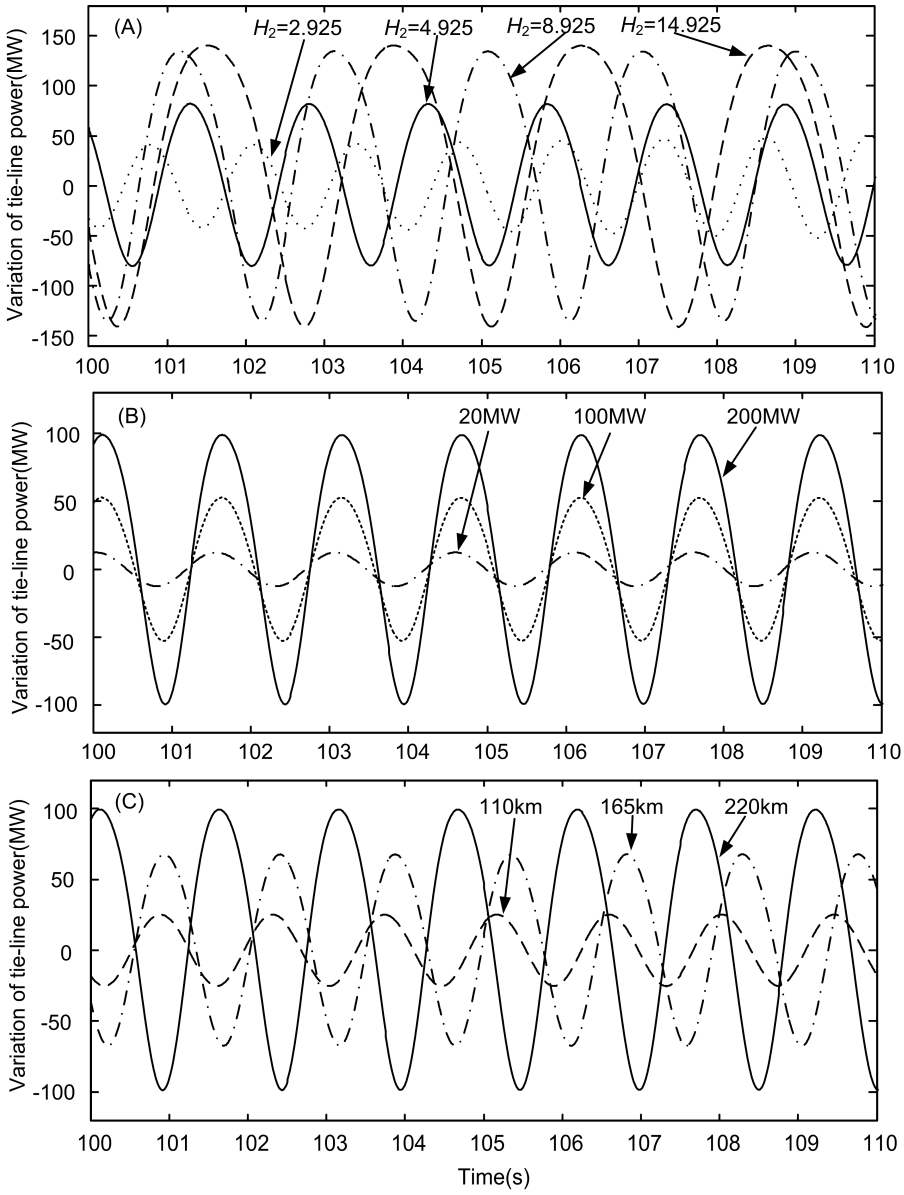

(B) Effect of Wind Power Penetration Capacity

Three cases are investigated by adjusting the penetration capacities of the wind farm to 200, 100 and 20 MW, respectively, and supposing the wind speed equals 8.5 m/s. For all cases, active power

productions are shifted between only G2 and the wind farm and thus the power flow in the tie-line remains unchanged.

Figure 9B shows that the magnitude is highest for 200 MW, lowest for 20 MW and f_{2n} remains the same. This can be explained by Equation (17), whereby as the capacity of a wind farm increases, the variations of wind power output increase and thus the magnitude of tie-line power oscillations increase. Equation (14) implies that the resonant frequency is the same for the tie-line power flow and system structure are unchanged.

(C) Effect of Tie-Line Impedance

The tie-line impedance can be varied by the length of the transmission line or changing the number of the tie circuits in service. Normally, the tie-line can be considered relatively "weak" as the length of the line increase or the number of the tie circuit decreases. To test the effect of tie-line impedance on tie-line power oscillations, the length of tie-line is adjusted to 110, 165 and 220 km, while keeping the tie-line power flow and the magnitudes of wind farm output variations unchanged.

Figure 9C shows that the resonant frequency is highest for 110 km and lowest for 220 km and the magnitude is highest for 220 km and lowest for 110 km. This can be explained by Equation (17) whereby as the tie-line length increases, the line impedance increases and the system damping decreases, so the resonant frequency f_{2n} decreases and the maximum magnitude of tie-line power oscillations increases. For the same reason, if the tie circuits in service are reduced, the impedance increases, and it will increase the risk of the tie-line power oscillations. The above simulations validate the theoretical analysis in Section 4.

6. Case II: WECC Interconnected System

Inter-area oscillations in a large realistic system are very complex. In this Section, the impacts of TSWS on tie-line power oscillations are tested in the WECC 127 bus system.

6.1. System Description

It is well known that the WECC system is prone to lightly dampened low frequency inter-area oscillations and some oscillations eventually contributed to the August 10, 1996 Western blackout [21]. The one line diagram and the geographical topology of the WECC system are depicted by Huang [22]. A schematic diagram is shown in Figure 10.

The WECC 127 bus system consists of 127 buses, 37 generators and 211 transmission lines. All the generators are represented by detailed synchronous generator models, and equipped with speed governors and exciters. The constant power load model is used. More detailed system data about WECC 127 bus system can be found in Huang's dissertation [22]. The full system model is implemented in the commercial power system analysis software (dynamic security assessment software, DSATools).

Figure 10. Schematic diagram of the WECC power system.

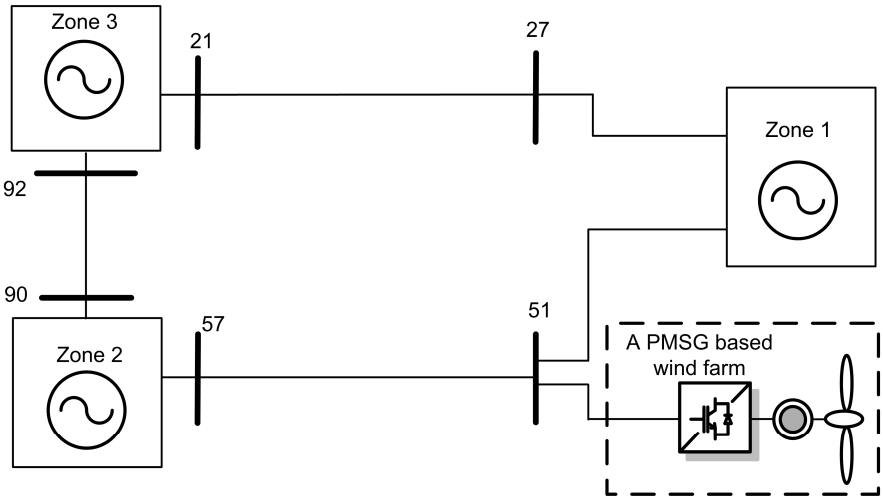

The system state matrix of the WECC system is formed by linearizing the system around an operating point, and the eigensolution of the state matrix contains information about all the oscillatory modes. There is an inter-area oscillation mode in which the western zone (Zone2) oscillates against the eastern zone (Zone1) with a frequency at 0.58 Hz (f_{2n}), so the tie-line which connects Zone 1 and Zone 2 (Bus 51 to Bus 57) is chosen. In order to test the potential largish effect of 3p oscillations on tie-power power oscillations, a PMSG-based wind farm with capacity of 500 MW is connected at Bus 51.

6.2. Simulation

The effects of TSWS on tie-line power oscillations at different wind speeds have been tested. Fourteen operating conditions, including wind speeds ranging from 5 to 11.5 m/s with 0.5 m/s steps, are considered. Figure 11 shows the plots of the tie-line power oscillations for four wind speeds: 5, 8 10 and 11.5 m/s.

Figure 11A shows that the magnitude of tie-line power oscillations is highest with a wind speed of 8 m/s and lowest with a wind speed at 5 m/s. The magnitude of tie-line power oscillations reaches nearly 30 MW with a wind speed at 8 m/s. Power systems operators should pay special attention to this phenomenon.

Furthermore, the amplification factors β_3 are used again to evaluate the impact of different operation points on tie-line power. The amplification factors at different wind speeds can be calculated by measuring $|\Delta P_m|$ and $|\Delta P_{line}|$. This case has two different natural frequencies f_{1n} (0.66 Hz) and f_{2n} (0.58 Hz) which is similar to Figure 5A. Figure 11B shows that, the tie-line power oscillations amplify the original mechanical power oscillations in the full range of operation points. When the wind speed equals to 8 m/s, the severest disturbance response appears in the tie-line. The tie-line power oscillations are amplified nearly four times. The maximum amplification happens at a frequency of 0.62 Hz, which is neither at f_{1n} nor f_{2n}. This could be explained that while f_{1n} is not equal to f_{2n}, the amplified factor of the tie-line power oscillation is a compound of two amplified factors of the subsystems. The above simulations for the selected cases can not only verify the result of frequency domain analysis, but also more accurately quantified the tie-line power oscillations by accounting for the system nonlinearities and harmonic frequency component.

Figure 11. Response of tie-line power and amplification with different wind speeds.

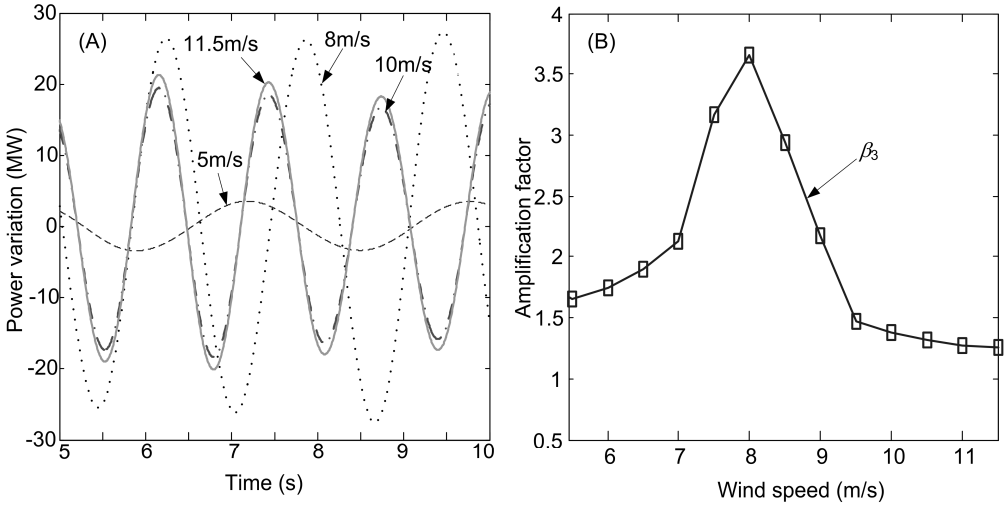

7. Conclusions

Special insight into the investigation of tie-line power oscillations induced by TSWS of a wind farm has been provided through frequency domain analysis which can provide information about the following three aspects: (1) the crucial frequency range where the disturbance will be amplified; (2) the expression of the maximum magnitude of tie-line power oscillations for assessing the worst situation; (3) qualitative parametric influence on the resonant magnitude of the tie-line power. On the other hand, time domain simulations have been conducted in the two-area four-generator system and the Western Electric Coordinating Council 127 bus system to validate the theoretical analysis. The results show that:

(a) The wind turbine system can be a source of forced oscillations to excite the low frequency oscillations in power systems, since the fundamental frequency of TSWS (f_{3p}) is typically in a range of 0.25 to 1.5 Hz. Particularly when the variable-speed wind turbine operates at medium-high wind speed, the resonance is more likely to happen.

(b) The TSWS of the wind farms can produce significant power oscillations in the tie-line of the interconnected systems, when the f_{3p} approaches the frequency of an inter-area mode.

(c) The soft shaft of the wind turbine can create a new peak which may also match inter-area mode and thereby cause highly amplified power oscillations in the tie-line. (e.g., in two-area four-generator system, the tie-line could suffer continuous power oscillations as large as 25 times the original mechanical power disturbance.)

(d) When the wind farm is connected to a small subsystem (low inertia) which transfers the power to a big subsystem (high inertia) through a relatively weak tie-line, the magnitude of the tie-line power resonance may increase.

From this study, it can be seen that the 3p oscillations of wind farm are not only harmful for the power quality but also even threaten the system stability in some cases. Based on this view, the 3p oscillations of wind farm are strongly suggested to be eliminated. Increasing the system damping, damping the shaft oscillations and eliminating the 3p power oscillations can be effective ways to attenuate tie-line power oscillations induced by TSWS.

Nowadays, variable-speed wind turbines are able to damp the 3p oscillations by adding some auxiliary controls, whereas there are still a large number of fixed-speed wind turbines existing in the system which still inject 3p oscillation power to the grid. Based on this background, this study also offers some information for disturbance source traceability. In real interconnected power systems, detailed quantitative studies are necessary to evaluate the resonant harm before the integration of a wind farm, especially for a fixed-speed wind farm.

Acknowledgments

This work is supported by the National Natural Science Foundation of China (50937002). Thanks are given to Peng Zhang and Peng He for their assistances with the simulations.

Conflicts of Interest

The authors declare no conflict of interest.

Appendix

Table A1. The Synchronous Generator Parameters in a Two-Area Four-Generator System.

Parameter	Value	Parameter	Value	Parameter	Value
Base rating	900 MVA	X_d	1.8	X''_d	0.25
Base voltage	20 kV	X_q	1.7	X''_q	0.25
$H(G_1,G_2)$	5.25	X_l	0.2	R_a	0.0025
$H(G_3,G_4)$	4.95	X'_d	0.3	T'_{d0}	8.0 s

Table A2. The Variable Speed Wind Turbine Parameters with PMSG.

Parameter	Value	Parameter	Value
Rated power	2 MW	Tower radius (a)	2 m
Rated voltage	0.69 kV	Distance from the blade origin to the tower midline (x)	4 m
Rated speed	15.5 rpm	wind turbine inertia	4.54 s
Stator resistance	0.03 pu	PMSG inertia	0.5 s
Stator direct reactance (X_d)	0.775 pu	Drive train shaft stiffness	0.5 pu/el.rad
Stator quadrature reactance (X_q)	0.775 pu	Wind turbine rotor radius	40 m
Stator leakage inductance	0.064 pu	Elevation of rotor hub	80 m
Magnetic strength	1 pu	Empirical wind shear exponent (α)	0.3

References

1. Rogers, G. *Power System Oscillations*; Kluwer Academic Publishers: Dordrecht, The Netherlands, 2000; pp. 3–10.
2. Kundur, P. *Power System Stability and Control*; McGraw-Hill Inc: New York, NY, USA, 1994; pp. 18–117, 813–816.
3. Rostamkolai, N.; Piwko, R.; Matusik, A. Evaluation of the impact of a large cyclic load on the LILCO power system using time simulation and frequency domain techniques. *IEEE Trans. Power Syst.* **1994**, *9*, 1411–1416.

4. Vournas, C.; Krassas, N.; Papadias, B. Analysis of Forced Oscillations in a Multimachine Power System. In Proceedings of the International Conference on Control, Edinburgh, UK, 25–28 March 1991; pp. 443–448.
5. Xiao, M.; Liang, Z. Analysis on the forced oscillation failure in China Southern Power Grid and its handling measures. *South. Power Syst. Technol.* **2012**, *6*, 51–54.
6. Dolan, D.; Lehn, P. Simulation model of wind turbine 3p torque oscillations due to wind shear and tower shadow. *IEEE Trans. Energy Convers.* **2006**, *21*, 717–724.
7. Sun, T.; Chen, Z.; Blaabjerg, F. Flicker study on variable speed wind turbines with doubly fed induction generators. *IEEE Trans. Energy Convers.* **2005**, *20*, 896–905.
8. Hu, W.; Zhang, Y.; Chen, Z.; Hu, Y. Flicker mitigation by speed control of permanent magnet synchronous generator variable-speed wind turbines. *Energies* **2013**, *6*, 3807–3821.
9. Ammar, M.; Joos G.; Impact of distributed wind generators reactive power behavior on flicker severity. *IEEE Trans. Energy Convers*. **2013**, *28*, 425–433.
10. Hughes, F.; Anaya-Lara, O.; Ramtharan, G.; Jenkins, N.; Strbac, G. Influence of tower shadow and wind turbulence on the performance of power system stabilizers for DFIG-based wind farms. *IEEE Trans. Energy Convers*. **2008**, *23*, 519–528.
11. Brownlees, S.; Flynn, D.; Fox, B.; Littler, T. The Impact of Wind Farm Power Oscillations on the Irish Power System. In Proceedings of the IEEE Power Technology, Lausanne, Switzerland, 1–5 July 2007; pp. 195–200.
12. Hu, W.; Su, C.; Chen, Z. Impact of Wind Shear and Tower Shadow Effects on Power System with Large Scale Wind Power Penetration. In Proceedings of the 37th Annual Conference on IEEE Industrial Electronics Society, Melbourne, Australia, 7–10 November 2011; pp. 878–883.
13. Akhmatov, V. *Induction Generators for Wind Power*; China Electric Power Press: Beijing, China, 2009; pp. 44–85.
14. Nielsen, J.N.; Akhmatov, V.; Thisted, J.; Grøndahl, E.; Egedal, P.; Frydensbjerg, M.N.; Jensen, K.H. Modelling and fault-ride-trough tests of Siemens wind power 3.6 MW variable-speed wind turbines. *Wind Eng.* **2007**, *31*, 441–452.
15. Chinchilla, M.; Arnaltes, S.; Burgos, J.C. Control of permanent-magnet generators applied to variable-speed wind-energy systems connected to the grid. *IEEE Trans. Energy Convers.* **2006**, *21*, 130–135.
16. Hu, W.; Chen, Z.; Wang, Y.; Wang, Z. Flicker mitigation by active power control of variable-speed wind turbines with full-scale back-to-back power converters. *IEEE Trans. Energy Convers.* **2009**, *24*, 640–649.
17. Yu, Y.; Min, Y.; Chen, L.; Zhang, Y. Analysis of forced power oscillation caused by continuous cyclical load disturbances. *Autom. Electric Power Syst.* **2010**, *34*, 7–11.
18. Yin, M.; Ge, X.; Zhang, Y. Major Problems Concerning China's Large-Scale Wind Power Integration. In Proceedings of the IEEE Power & Energy Society General Meeting, Detroit, MI, USA, 24–29 July 2011; pp. 1–6.
19. Klein, M.; Rogers, G.; Kundur, P. A fundamental study of inter-area oscillations in power systems. *IEEE Trans. Power Syst.* **1991**, *6*, 914–921.

20. Tripathy, P.; Srivastava, S.; Singh, S. A modified TLS-ESPRIT-based method for low-frequency mode identification in power systems utilizing synchrophasor measurements. *IEEE Trans. Power Syst.* **2011**, *26*, 719–727.
21. Kosterev, D.; Taylor, C.; Mittelstadt, W. Model validation for the August 10, 1996 WSCC system outage. *IEEE Trans. Power Syst.* **1999**, *14*, 967–979.
22. Huang, L. Electromechanical Wave Propagation in Large Electric Power Systems. Ph.D. Thesis, Virginia Polytechnic Institute and State University, Blacksburg, VA, USA, 2003.